

# A Novel Atlas-Based Strategy for Understanding Cardiac Dysfunction in Patients with Congenital Heart Disease

Sara Salehyar<sup>1, †</sup>, Nickolas Forsch<sup>1, †, \*</sup>, Kathleen Gilbert<sup>2, 3</sup>, Alistair A. Young<sup>3, 4</sup>, James C. Perry<sup>5</sup>, Sanjeet Hegde<sup>5</sup>, Jeffrey H. Omens<sup>1, 6</sup> and Andrew D. McCulloch<sup>1, 6</sup>

<sup>1</sup>Department of Bioengineering, University of California San Diego, La Jolla, USA.

<sup>2</sup>Auckland Bioengineering Institute, University of Auckland, Auckland, New Zealand.

<sup>3</sup>Department of Anatomy and Medical Imaging, University of Auckland, Auckland, New Zealand.

<sup>4</sup>Department of Biomedical Engineering, King's College London, United Kingdom.

<sup>5</sup>Department of Pediatrics, University of California San Diego, La Jolla, USA.

<sup>6</sup>Department of Medicine, University of California San Diego, La Jolla, USA.

<sup>†</sup>These authors contributed equally to this work.

\*Corresponding Author: Nickolas Forsch. Email: nforsch@eng.ucsd.edu.

**Abstract:** Tetralogy of Fallot (TOF) is the most common form of cyanotic congenital heart disease. Infants diagnosed with TOF require surgical interventions to survive into adulthood. However, as a result of postoperative structural malformations and long-term ventricular remodeling, further interventions are often required later in life. To help identify those at risk of disease progression, serial cardiac magnetic resonance (CMR) imaging is used to monitor these patients. However, most of the detailed information on cardiac shape and biomechanics contained in these large four-dimensional (4D) data sets goes unused in clinical practice for lack of efficient and comprehensive quantitative analysis tools. While current global metrics of cardiac size and function, such as indexed ventricular mass and volumes, can identify patients at risk of further complications, they are not adequate to explain the underlying mechanisms causing the postoperative malfunctions, and help cardiologists plan optimal personalized treatments. We are proposing a novel approach that uses 4D ventricular shape models derived from CMR imaging exams to generate statistical atlases of ventricular shape and finite-element models of ventricular biomechanics to identify specific features of cardiac shape and biomechanical properties that explain variations in ventricular function. This study has the potential to discover novel biomarkers that precede adverse ventricular remodeling and dysfunction.

**Keywords:** Tetralogy of fallot; statistical shape atlas; principle component analysis; left ventricular biomechanics; finite-element modeling; adult congenital heart disease

## 1 Introduction

Congenital heart disease (CHD) is the most common type of birth defect. With the improvements in the management of CHD, infants born with these cardiac malformations can now survive into adulthood [1]. Among these congenital heart defects, tetralogy of Fallot (TOF), characterized by four anatomical defects (pulmonary stenosis, right ventricular hypertrophy, ventricular septal defect, and an overriding aorta), is the most common heart lesion accounting for approximately 10% of all congenital cardiac malformations [2]. These issues are typically addressed by surgery after birth, however, these surgical repairs often lead to pulmonary regurgitation (PR) by the second or third decade of life that can lead to right

ventricular (RV) enlargement and dysfunction, consequent left ventricular (LV) remodeling and, ultimately, heart failure [3-6].

In patients with repaired tetralogy of Fallot (rTOF), cardiac magnetic resonance (CMR) imaging is the gold standard for clinical decision support because of its ability to quantify ventricular size and function [7]. Despite the wealth of information available in four-dimensional (4D) cardiac shape and wall motion in CMR, only a small set of measurements of global cardiac volume and size are used by cardiologists for determining the time of further interventions in rTOF patients. Shape atlases derived from surface registration methods provide a high spatial resolution of cardiac morphology. The application of dimensionality-reduction techniques, such as principal component analysis (PCA), to three-dimensional (3D) ventricular shape can derive orthogonal modes of shape and function in an unbiased framework. Recent studies of ventricular morphology and function have adopted statistical shape modeling as a method of atlas generation in both congenital and asymptomatic cohorts, demonstrating an association of atlas-based shapes to risk factors and dysfunction [8-10].

This short paper is a demonstration of the methods developed to understand the underlying mechanisms causing the postoperative malfunctions in rTOF by using the 4D information in CMR. In Section 2, the statistical atlas approach and ventricular finite-element (FE) modeling are briefly described. In Section 3, preliminary results related to the clinical application of statistical shape atlases have been included. The results of the ventricular FE modeling and more elaborate and advanced results of the statistical atlases of ventricular shape will be included in our future publications.

## **2 Methods**

### ***2.1 Study Cohort and Clinical Data***

CMR image data of patients with rTOF were obtained from the CHD Cardiac Atlas Project (CAP) database (<http://www.cardiacatlas.org>), which integrates clinical data and derived shape models of patients with congenital defects. This study used retrospective CMR data from 99 patients with rTOF. CMR datasets were obtained with informed consent and de-identified and contributed to the CHD CAP database following approval of the local institutional review boards at the University of California San Diego (La Jolla, CA, USA) and University of Auckland (Auckland, New Zealand). CMR measurements of the LV were made using custom software (CIM, Auckland, New Zealand). RV volume and function data from CMR measurements were collected for a subset of 11 patients with rTOF who had serial CMR data.

### ***2.2 Statistical Atlases of LV Shape***

Methods for generating shape models of the LV and statistical atlases of ED shape variation have been previously described in [8] and [9]. The process involves a geometric fit analysis using guide-point modeling software (CIM, Auckland, New Zealand). For each case, a 3D shape model is fit to endocardial and epicardial surface contours, and overall model alignment is achieved using fiducial anatomical landmarks. An atlas of LV ED shape was derived by applying PCA to 3D coordinate points from the endocardial and epicardial surfaces of the shape models from the rTOF patient group. This study used a previously derived atlas of LV ED shape in an asymptomatic control population for comparison to the congenital atlas [8].

### ***2.3 Analysis of Shape Atlas and Clinical Data***

To quantify differences between ED shape modes derived in the atlas of patients with rTOF and those from the asymptomatic control atlas, we used an analysis from Krzanowski to calculate vector projections between the first twenty principal components of both atlases [11]. This calculation produces a scalar between 0, indicating orthogonal shape modes, and 1, indicating equivalent shape modes.

A subset of 11 rTOF patients were used in a longitudinal study of LV and RV remodeling. To explore the potential value of novel atlas-based shape modes in predicting changes in LV and RV volume and function, regression analysis was used to test for correlations between various baseline parameters and the

change in indexed RV and LV end-diastolic volume (EDVi), end-systolic volume (ESVi), stroke volume (SVi), and ejection fraction (EF). The baseline parameters consisted of RV and LV CMR parameters as well as shape mode z-scores from the rTOF ED atlas. Statistical analyses were performed using R Studio (R Studio Inc., Boston, MA).

### 2.4 Finite-Element Models of Ventricular Biomechanics

Ventricular FE models enable the estimation of muscle passive stiffness, active properties, and wall stresses. In this study, ventricular geometry was generated from epicardial and endocardial surfaces of the atlas-based shapes, and cubic-Hermite FE meshes were generated accordingly. The load-free geometry and passive material properties of the average rTOF patient were estimated using the iterative method proposed in [12]. In the strained ED configuration, the active forces will be adjusted such that the ventricular shape and volume from the FE model will match the measured end-systole shape and volume. In this model, the first mode of ED shape from the rTOF atlas will be varied to test for potential mechanisms of dysfunction due to variations in this rTOF-specific shape mode.

## 3 Results

### 3.1 Comparison Between ED Shape Atlases of rTOF and Asymptomatic Groups

An atlas of statistical shape variation at ED was derived using PCA of the LV shapes of the rTOF patients, resulting in five shape modes explaining over 75% of total variation in the rTOF patients. Systematic comparison of the first twenty ED shape modes of the rTOF and control atlases identified the first mode of the rTOF group (Fig. 1) as having the lowest similarity to an ED mode of the control atlas; rTOF mode 1 had the highest degree of orthogonality to modes of the control atlas with a maximum vector projection value of 0.16. This first mode explained 26% of all ED shape variation in the rTOF patients.

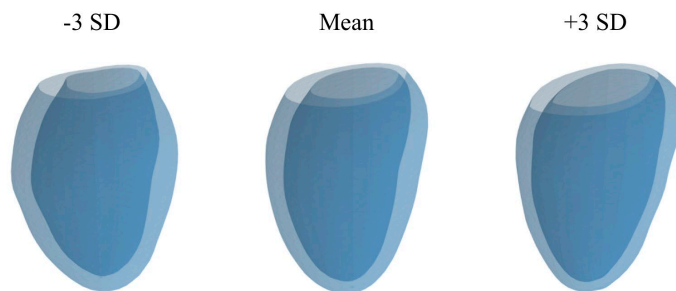


**Figure 1:** Shape variation of the first mode of the rTOF end-diastolic atlas

### 3.2 Prediction of LV and RV Remodeling

The first shape mode of the rTOF atlas was the best predictor among all baseline variables for three of the eight response variables ( $\Delta$ LVESVi,  $\Delta$ LVEF, and  $\Delta$ RVESVi) and significantly correlated with four of the eight ( $\Delta$ LVESVi,  $\Delta$ LVEF,  $\Delta$ RVEDVi, and  $\Delta$ RVESVi;  $p < 0.05$ ) after controlling for age and time between CMR examinations (Tab. 1). The strongest predictions were between baseline rTOF shape mode 1 and  $\Delta$ LVESVi ( $R^2 = 0.80$ ,  $p < 0.01$ ) and baseline LVESVi and  $\Delta$ RVEDVi ( $R^2 = 0.80$ ,  $p < 0.01$ ).

**Table 1:** Correlation of baseline parameters to changes in ventricular volumes and function

Baseline predictor variable	Mean <sup>†</sup> (N = 11)	Response variable <sup>‡</sup>							
		ΔLVEDVi	ΔLVESVi	ΔLVSVi	ΔLVEF	ΔRVEDVi	ΔRVESVi	ΔRVSVi	ΔRVEF
LVEDVi, mL/m <sup>2</sup>	83.3 ± 7.7	0.29	0.48	0.11	0.42	0.75*	0.51	0.75*	0.41
LVESVi, mL/m <sup>2</sup>	30.8 ± 5.3	0.28	0.49	0.29	0.59	<b>0.80**</b>	0.55	<b>0.78*</b>	0.44
LVSVi, mL/m <sup>2</sup>	52.5 ± 5.4	0.34	0.39	0.14	0.28	0.54	0.37	0.56	0.45
LVEF, %	63.1 ± 4.6	0.30	0.45	<b>0.34</b>	0.56	0.67*	0.47	0.65*	0.47
RVEDVi, mL/m <sup>2</sup>	140 ± 32	0.28	0.39	0.09	0.28	0.53	0.41	0.59	0.53
RVESVi, mL/m <sup>2</sup>	62.6 ± 17	0.33	0.48	0.08	0.32	0.53	0.44	0.61	<b>0.59</b>
RVSVi, mL/m <sup>2</sup>	77.7 ± 18	0.34	0.40	0.12	0.29	0.52	0.38	0.56	0.46
RVEF, %	55.6 ± 5.1	<b>0.70*</b>	0.77	0.14	0.42	0.53	0.44	0.60	0.57
rTOF ED mode 1	0.40 ± 0.6	0.44	<b>0.80**</b>	0.09	<b>0.65*</b>	0.68*	<b>0.74*</b>	0.56	0.47

\* $p < 0.05$ , \*\* $p < 0.01$ .

<sup>†</sup>Values represented as Mean ± SD.

<sup>‡</sup>Bold values indicate the best predictor variable for each response variable.

#### 4 Conclusions

Shape modeling of the LV in rTOF revealed unique modes of ED shape that were often better than conventional CMR parameters in predicting RV and LV remodeling. This study demonstrates the clinical utility of statistical shape modeling in the context of CHD, the ultimate goal of which is to discover novel biomarkers of shape and function that precede long-term adverse ventricular remodeling and dysfunction.

#### References

- Gurvitz M, Burns KM, Brindis R, Broberg CS, Daniels CJ et al. Emerging research directions in adult congenital heart disease: a report from an NHLBI/ACHA working group. *Journal of the American College of Cardiology* **2016**, 67(16): 1956-1964.
- Brickner ME, Hillis LD, Lange RA. Congenital heart disease in adults. *New England Journal of Medicine* **2000**, 342(5): 334-342.
- Aboulhossn JA, Lluri G, Gurvitz MZ, Khairy P, Mongeon FP et al. Left and right ventricular diastolic function in adults with surgically repaired tetralogy of fallot: a multi-institutional study. *Canadian Journal of Cardiology* **2013**, 29(7): 866-872.
- Broberg CS, Aboulhossn J, Mongeon FP, Kay J, Valente AM et al. Prevalence of left ventricular systolic dysfunction in adults with repaired tetralogy of fallot. *American Journal of Cardiology* **2011**, 107(8): 1215-1220.
- Khairy P, Aboulhossn J, Gurvitz MZ, Opatowsky AR, Mongeon FP et al. Arrhythmia burden in adults with surgically repaired tetralogy of fallot: a multi-institutional study. *Circulation* **2010**, 122(9): 868-875.
- Valente AM, Gauvreau K, Assenza GE, Babu-Narayan SV, Schreier J et al. Contemporary predictors of death and sustained ventricular tachycardia in patients with repaired tetralogy of fallot enrolled in the INDICATOR cohort. *Heart* **2014**, 100(3): 247-253.
- Villafañe J, Feinstein JA, Jenkins KJ, Vincent RN, Walsh E P et al. Hot topics in tetralogy of fallot. *Journal of the American College of Cardiology* **2013**, 62(23): 2155-2166.
- Medrano-Gracia P, Cowan BR, Ambale-Venkatesh B, Bluemke DA, Eng J et al. Left ventricular shape variation in asymptomatic populations: the multi-ethnic study of atherosclerosis. *Journal of Cardiovascular Magnetic Resonance* **2014**, 16(1): 56.

9. Farrar G, Suinesiaputra A, Gilbert K, Perry JC, Hegde S et al. Atlas-based ventricular shape analysis for understanding congenital heart disease. *Progress in pediatric cardiology* **2016**, 43: 61-69.
10. Gilbert K, Forsch N, Hegde S, Mauger C, Omens JH et al. Atlas-based computational analysis of heart shape and function in congenital heart disease. *Journal of Cardiovascular Translational Research* **2018**, 11(2): 123-132.
11. Krzanowski WJ. Between-groups comparison of principal components. *Journal of the American Statistical Association* **1979**, 74(367): 703-707.
12. Krishnamurthy A, Villongco CT, Chuang J, Frank LR, Nigam V et al. Patient-specific models of cardiac biomechanics. *Journal of Computational Physics* **2013**, 244: 4-21.